Marine Pollution Bulletin 203 (2024) 116483

Contents lists available at ScienceDirect

Marine Pollution Bulletin

journal homepage: www.elsevier.com/locate/marpolbul

Source-specific geochemical and health risk assessment of anthropogenically induced metals in a tropical urban waterway

Md Kamal Hossain [a,b,*], Fahima Islam [a], Kowshik Das Karmaker [a], Umme Sarmeen Akhtar [c], Afsana Parvin [a], Afroza Parvin [a], Mohammad Moniruzzaman [a,b], Badhan Saha [a], Priyanka Dey Suchi [a], Md Anwar Hossain [d], Md Aftab Ali Shaikh [e]

[a] *BCSIR Laboratories Dhaka, Bangladesh Council of Scientific and Industrial Research (BCSIR), Dhaka - 1205, Bangladesh*
[b] *Central Analytical Research Facilities (CARF), Bangladesh Council of Scientific and Industrial Research (BCSIR), Dr. Qudrat-E-Khuda Road, Dhanmondi, Dhaka - 1205, Bangladesh*
[c] *Institute of Glass and Ceramic Research and Testing (IGCRT), Bangladesh Council of Scientific and Industrial Research (BCSIR), Dhaka - 1205, Bangladesh*
[d] *Planning and Development Division, Bangladesh Council of Scientific and Industrial Research (BCSIR), Dhaka - 1205, Bangladesh*
[e] *Bangladesh Council of Scientific and Industrial Research (BCSIR), and Department of Chemistry, Dhaka University, Dhaka - 1000, Bangladesh*

A R T I C L E I N F O

Keywords:
Sediment
Trace metals
Geochemical indices
Chemometric analyses
Health hazards
Southern shoreline
Bangladesh

A B S T R A C T

Thorough deliberation is necessary to safeguard the tropical urban streams near the shoreline from human interference, as it is becoming a notable environmental danger. Consequently, an in-depth study was carried out on a significant urban waterway located on the southern seashore of Bangladesh, which is positioned in the Bengal delta, renowned as the largest delta in the globe. The current investigation assesses the potential health hazards associated with trace metals (Hg, Cu, As, Pb, Ni, Zn, Cd, Cr, Fe, and Mn) and uses chemometric analysis to determine where they originate. Likewise geochemical methods are used to analyze the levels of trace metal enrichment and pollution in the sediments of the river. Almost all of the elements' mean concentrations were observed to be within the standard limits. The findings not only demonstrate the extent of trace metal contamination but also the health threats that it poses to the public (male, female, and children) by polluting the sediment. For all age groups of people, the hazard index was <1, suggesting there was no non-carcinogenic threat. Regardless of age and sex, exposure occurred in descending order: ingestion $>$ dermal $>$ inhalation. Total carcinogenic risk (TCR) values for males, females, and children were 1.45E-05, 1.56E-05, and 1.34E-04, respectively, recommending that children are at greater vulnerability than adults. The geochemical approach and chemometric analysis corroborate the human-induced impact of trace metal loading in the sediment of the waterway, which is predominantly caused by the oil industry, domestic garbage, and untreated waste discharge.

1. Introduction

Being the world's largest delta, the Ganges-Brahmaputra Delta, also referred to as the Bengal Delta, is home to unique biodiversity. Salt intrusion, climate change and other anthropogenic factors are making the environment of the delta, particularly the southwestern Bangladesh more vulnerable (Akter et al., 2020). Spilling tons of raw sewage into waterways is extremely hazardous to both the environment and human health, as it introduces all sorts of unpleasant substances into the water that should not be there (Karmaker et al., 2024). According to research, pollution originating from treated and untreated sewage has become the most serious threat to water biodiversity. Trace metals, when found in waterbodies, can act as markers of anthropogenic or natural causes that affect the quality of aquatic habitats, and as a result, they are now a major problem worldwide (Bai et al., 2012). Trace metals with high ecological precedence are considered pollutants as they cannot be eliminated from water through self-purification (Ghrefat and Yusuf, 2006). Sediments are the greatest metal reservoir in aquatic environments (Zhang et al., 2017), with suspended particulate matter and sediments containing over 90 % of the trace metal burden (Zheng et al., 2008).

Sediments have been often employed as indicators of aquatic environmental quality to assess metal contamination in natural water because they have a substantial potential for gathering extremely rare to

* Corresponding author at: BCSIR Laboratories Dhaka, Bangladesh Council of Scientific and Industrial Research (BCSIR), Dhaka - 1205, Bangladesh.
E-mail address: kamalhossain@bcsir.gov.bd (M.K. Hossain).

https://doi.org/10.1016/j.marpolbul.2024.116483
Received 9 February 2024; Received in revised form 25 April 2024; Accepted 7 May 2024

undetectable levels of trace metals from underlying waters (Soares et al., 1999). However, it is impractical to estimate how much of an impact these metals would have on the environment based on their concentrations in sediments (Sekhar et al., 2004). As a consequence, to scrutinize the potential environmental consequences and toxicity of trace metals, geochemical speciation has drawn special attention (Islam et al., 2018a).

Adverse physiological effects may result from either direct or indirect assimilation of trace metals in the human body from contaminated sediments, as fish uptake these more than from water and can travel up the food chain. People may come into close proximity of waters near catchment areas harboring contaminated sediment due to activities like bathing, cooking, cleaning and other recreational activities, having a detrimental effect on human wellness (Jolly et al., 2023). Because of negative traits of tiny chemicals, i.e. persistence, toxicity, biomagnifications and bioaccumulation, they may be a significant source of peril to human well-being (Zahra et al., 2014; Hossain et al., 2021; Jolly et al., 2023). Intake of trace metals has been linked to numerous detrimental human illnesses including cancer, heart and lung diseases resulting in mortality in some cases (Ghrefat and Yusuf, 2006). Lead, mercury, arsenic, and cadmium are the trace metals that are most frequently implicated in poisoning in humans (Parvin et al., 2023). Some metals, like zinc, copper, chromium, iron, and manganese, are needed by the body in minimal quantities, but in excessive dosages can be poisonous.

Bangladesh features one of the world's largest active deltas and is mostly reliant on waters from the rivers for agriculture and other economic endeavors. The country is being jeopardized by increasing natural disasters and uncertainties resulting from global warming, sea level rise, growing populations, and socioeconomic development. Bangladesh recently developed the Bangladesh Delta Plan 2100, which prioritizes long-term adaptive strategies (Hossain and Majumder, 2018).

The Kirtankhola River, adjacent to Barisal town and second in terms of area next to Narayangonj river-port in Bangladesh, has a significant role in aquatic ecosystems. It is an important hub of transportation which connects different regions of Bangladesh through waterways. The river was extraordinarily broad, deep, and furious when the British were in power. However, over a century, char development caused the waterway's width to fall by approximately 50 %. Furthermore, its water-based assets and abundance of freshwater are critical to the life, farming, and biodiversity of a broad area. The river, on the other hand, swallows hazardous trash from a variety of manufacturing plants, including battery manufacturers, painting-related workstations, agrochemical producers, and so on (Ali et al., 2022a). As a result, in the context of environmental evaluation and enactment, an illustration of the geographical background or foundational levels of trace metals needs to be provided (Jiang et al., 2013). Quite a few research has been carried out on the prospect of contamination of heavy metals in the Shitalakshya River (Jolly et al., 2023), Brahmaputra River (Hossain, 2022), Old Brahmaputra River (Shorna et al., 2021), Buriganga River (Islam et al., 2018a), Feni River estuary (Islam et al., 2018b), Meghna River (Bhuyan et al., 2017), and Karnaphuli River (Ali et al., 2016) sediments; in addition to the accumulation of dangerous metals in commercial fish from the Kirtankhola River (Ali et al., 2022a). These studies surprisingly ignored the significant issue of the Kirtankhola River sediment's potential danger to ecological and human health. Hence, the current study will use different parameters and approaches to assess the impacts on human health as well as the ecological consequences and detection of both naturally occurring and man-made sources of trace metals in the Kirtankhola River, Barisal. The research goals are as follows: (1) to determine the concentration of ten important trace metals; (2) to figure out the ecological status of the sediment-bound trace metals; (3) to pinpoint the most likely origin of trace metals using chemometric approaches; and (4) to assess the risk to human health posed by routes of exposure – dermal contact, inhalation and ingestion. The findings will provide new insight into the human health impacts and anthropogenic influences of the investigated waterway.

2. Materials and methods

2.1. Description of the study area and sampling

The Kirtankhola River port is one of the most important ones in Bangladesh housed near Barisal town and it consists of diverse ecosystems with much aquaculture impending. The Kirtankhola River (Latitude 22° 74′ 32″ N and longitude 90° 42′ 09″ E) emerges from Sayeshtabad in Barisal District and flows to Gajalia near Gabkhan Khal (canal). The river's overall length is about 160 km. The divisional town of Barishal is located on its bank. Sediment samples were collected using an Ekman dredge from the Kirtankhola River. Fifteen stations along the river were chosen for analysis, as displayed in Fig. 1. These stations are Mohammadpur (S1), Rasulpur Mohona (S2), Rasulpur Ghat (S3), Balurghat (S4), Kheya Ghat (S5), Batar Khal (S6), Muktijodda Park 1 (S7), Muktijodda Park 2 (S8), KDC (S9), Chandmari (S10), Jamuna Oil Depot (S11), 30 Godown Shahid Sriti Shoudho (S12), Char Kauwa 1 (S13), Char Kauwa 2 (S14), Char Kauwa 3 (S15). In total, 15 sediments (0–10 cm) from the inter-tidal zone were collected (S1 to S15) simultaneously during low tide with triplicates of each station during early December 2020. Sampling began from Mohammadpur (22° 70′ 34″ N and 90° 38′ 14″ E) and ended at 30 Godown Shahid Sriti Shoudho (22° 67′ 83″ N and 90° 36′ 51″ E). After collection, the samples were subsequently placed in polythene bags, tagged with the sample location name, and finally carried to the Laboratories. Sediment samples were air dried and thoroughly pulverized, strained using a 2 mm strainer, and stored for further chemical analysis. Sediment grain size distribution and organic matter content were analyzed, and further details are given in supporting information (Supplementary Table S1 and S2). The texture class of sediment was silty clay.

2.2. Digestion procedure and chemical analysis

The Atomic Absorption Spectrophotometer (Model: AA-700, Shimadzu, Japan) was used to analyses environmental samples according to standard analytical procedures (Supplementary Table S3). The glassware was washed carefully with an acid solution and then with distilled water. All the sample procedures strictly followed the standard digestion procedure of the US-EPA 3050B method. Typically, in a 50-ml beaker, 2 g of sediment specimens were taken. Afterwards, approximately 10 ml of HNO_3 (conc.) acid was poured into the beaker. A watch glass was placed in the beaker's mouth and then set on a hot plate. To prevent violent responses, the temperature was first kept at around 40 °C for one hour. The temperature was then kept at 140 °C for another 3 h. After cooling the samples, 5 ml of H_2O_2 was added to them, which was then heated until a white fume was detected. Following that, the solutions were cooled and filtrated into a 50-ml volumetric flask with Whatman No. 44 filter paper, rinsing the residue. Each sample was brought up to date by adding deionized water. An AAS standard for each element was chosen from Sigma-Aldrich TraceCERT CRM 250ML 1000 mg/l ± 4 mg/l (Trace SELECT is a registered trademark of Honeywell Specialty Chemicals Seelze GmbH), a product of Switzerland, and used to calibrate the curve at ppm levels except for As and Hg at ppb levels.

2.3. Quality control (QC) and quality assurance (QA)

Throughout the research procedure, analytical-grade chemicals and reagents were employed with further purification. All glassware used in this experiment was cleaned and rinsed with ultrapure acid and water to reduce the possibility of contamination during sample preparation and analytical operations. Deionized ultrapure water (TKA Milli-Q Ultra-Pure Water System, Germany) has been utilized to prepare every additional reagent and standard for calibration. A standard reference material SRM 2702 (for inorganics in marine Sediment) from the National

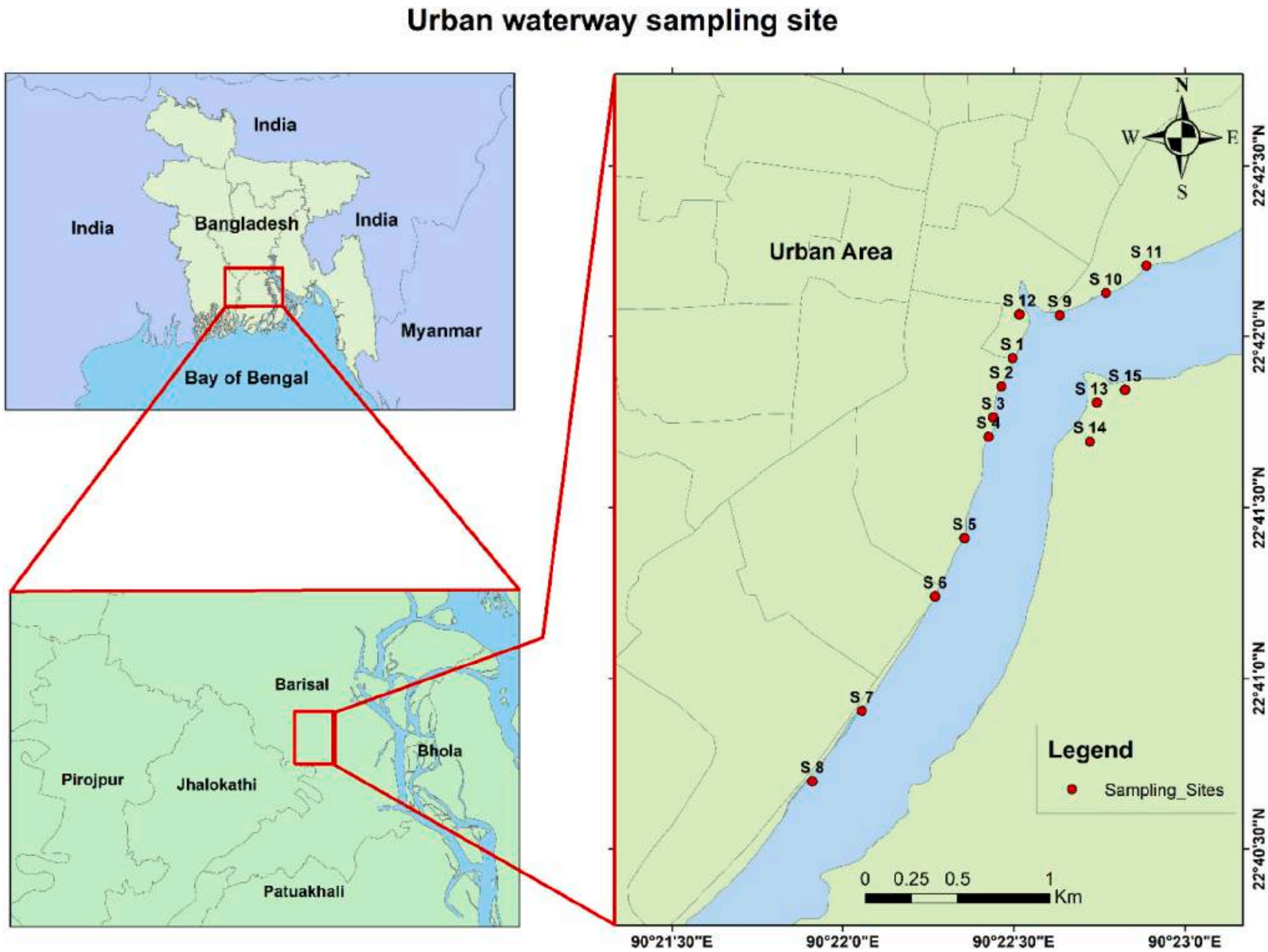

Fig. 1. Map showing the Kirtankhola River of Bangladesh with sampling points.

Institute of Standards (NIST) was used to check the recovery percentage of elements in the sample and showed 97–103 % recovery for significant elements (Supplementary Table S4). We accepted a five-point calibration variance with $R^2 > 0.9998$, 5–10 % of the maximum relative standard deviation (RSD), a minimum of three replications to confirm the stability of the instrument, a detection limit (DL) of three times, and a quantification limit (QL) 10 times response of greater than the background noise to specific metals. The procedure blanks, SRM recoveries, and spike recoveries were performed as part of the quality control process to minimize error, followed by ISO/IEC 17025:2017. The concentrations of trace metals were corrected by recovery and blank sample analysis.

2.4. Geochemical appraisal

Several geochemical indices have been developed to distinguish natural metal sources from human-induced sources as well as assess the human-caused contamination status. Table 1 contains details for those indexes.

2.5. Chemometric approach

Chemometrics is an assortment of approaches for designing and analyzing laboratory experiments, the majority of which are chemical in nature (Brereton, 1990). Multivariate chemometric approaches, including principal component analysis (PCA) and cluster analysis (CA), are increasingly being used for environmental investigations, including the detection and monitoring of trace metals (Chabukdhara and Nema, 2012). Previous research confirmed that multivariate analysis generates valid conclusions about the sources of trace metals (Chabukdhara and Nema, 2012; Sungur and Özcan, 2015). Groups or clusters of similar sites are found using cluster analysis, which is based on similarities within a class and differences between classes. Principal components, or PCAs, are linear combinations of the original variables that are created from the original variables using a sophisticated pattern identification analytical technique (Chabukdhara and Nema, 2012). To identify the correlations between metals, Pearson correlation analysis was used. The SPSS 19.0 software package (IBM SPSS Inc., Chicago, USA) for Windows was used to perform all statistical analyses on the data.

2.6. Human health risk assessment

Excessive metal concentrations can typically impact human health through three main pathways: ingestion, inhalation, and dermal absorption (Hu et al., 2017). The following Eqs. (1)–(3) can be used to calculate exposure through these routes for non-carcinogenic effects on human health (adult male, adult female, and children) (Ali et al., 2022b). Details of the parameters are presented in Table 2

$$CDI_{dermal} = \frac{CS \times SA \times AF \times EF \times ED \times ABS}{BW \times AT \times 10^6} \quad (1)$$

Table 1
Geochemical approaches with classification.

Index	Formula	Classification	References
Geo-accumulation Index (I_{geo})	$I_{geo} = log_2\left[\frac{C_n}{1.5\,B_n}\right]$ Cn is the concentration of the metals observed in sediment samples. Bn is the geochemical background value of a given metal in the shale and the factor 1.5 means the "background matrix correlation value" responsible for lithospheric differences.	The geo- accumulation index consists of seven classes: < 0: practically unpolluted; 0–1: unpolluted to moderately polluted; 1–2: moderately polluted; 2–3: moderately to strongly polluted; 3–4: strongly polluted; 4–5: strongly to extremely polluted; > 5: extremely polluted	Rakib et al. (2021) Müller (1969)
Contamination Factor (CF)	$CF = \frac{C_n}{B_n\ (Shale)}$ Cn sample is the concentration of a given metal in coast sediment, and Bn Shale is the geochemical background value of a given metal in the shale	CF < 1: low contamination; 1 ≤ CF < 3: moderate contamination; 3 ≤ CF ≤ 6: considerable contamination; CF > 6: very high contamination	Hakanson (1980) Turekian and Wedepohl (1961)
Enrichment Factor (EF)	$EF = (C_M/C_{Fe})_{sample}/(C_M/C_{Fe})_{background}$ Where (C_M/C_{Fe}) sample is the ratio of heavy metal (C_M) to that of iron (C_{Fe}) in the sediment sample, and (C_M/C_{Fe}) is the geochemical background value of metal to Fe ratio. Generally, Al and Fe are most often used as reference ones. In this study, we did not analyze Al concentration, and Fe was chosen as the reference material of normalization.	EF < 1 indicates no enrichment; 1 < EF < 3 indicates no enrichment; 3 < EF < 5 indicates mild enrichment; 5 < EF < 10 indicates moderately severe enrichment; 10 < EF < 25 indicates severe enrichment; 25 < FE < 50 indicates very severe enrichment; and EF > 50 indicates extremely severe enrichment	Birch and Olmos (2008)
Pollution Load Index (PLI)	$PLI = \sqrt[n]{(CF1 \times CF2 \times CF3 \times CF4 \times \ldots\ldots CFn)}$ Pollution Load Index (PLI) can be used for assessment comparison of contamination status among the study sites. The PLI is defined as the nth root of the multiplications of the contamination factor of metals (CF).	PLI < 1: No pollution; PLI > 1: polluted	Maanan et al. (2015) Tomlinson et al. (1980)
Potential Ecological Risk Index (RI)	$RI = \sum_{i=1}^{n} E_r^i$ $E_r^i = T_r^i \times CF$ E_r^i is the potential ecological risk factor and T_r^i is the toxic response factor of studied metals. T_r^i was determined for Zn = 1, Cu = Pb = Ni = 5, As = 10, Cr = 2, Cd = 30 and Hg = 40	$E_r^i < 40$: Low ecological risk $E_r^i \le 80$: Moderate ecological risk; $80 < E_r^i \le 160$: Appreciable ecological risk; $160 < E_r^i \le 320$: High ecological risk; $E_r^i > 320$: Serious ecological risk, And RI < 150: Low pollution; RI: 150 < RI <300: Considerable pollution; RI: 300 < RI < 600: High pollution; RI ≥ 600: Very high pollution	Ke et al. (2015) Suresh et al. (2011) Hakanson (1980)

$$CDI_{ingestion} = \frac{CS \times EF \times ED \times IRS}{BW \times AT \times 10^6} \quad (2)$$

$$CDI_{inhalation} = \frac{CS \times Inh \times EF \times ED}{BW \times PEF \times AT} \quad (3)$$

Where CDI_{dermal} = chronic daily intake via dermal contact (mg/kg/day); $CDI_{ingestion}$ = chronic daily ingestion of metals (mg/kg/day); and $CDI_{inhalation}$ = intake of metals via inhalation (mg/kg/day). To convert from kg to mg, 10^6 was utilized as a conversion factor.

As proposed by the guideline to assess health risk (USEPA, 2011), the hazard quotient (HQ) is a determinant of non-carcinogenic health consequences caused by metal exposure to contaminated sediment, and it may be calculated by the Eq. (4):

$$HQ = \frac{CDI}{RfD} \quad (4)$$

The ratio of CDI (mg/kg/d) to reference dose (RfD) (mg/kg/d) is HQ. The RfD values (mg/kg/d) for each metal alongside their exposure pathways are listed in Table 3.

HI is represented as the summation of HQ of the three major pathways for the analyzed metals. The assessment equation for HI is as follows:

$$HI = \sum HQ = HQ_{dermal} + HQ_{ingestion} + HQ_{inhalation} \quad (5)$$

Values of HI < 1 attribute no considerable risk of non-carcinogenic consequences, whereas HI > 1 attribute the possibility of non-carcinogenic effects on humans (Zhao et al., 2018).

Using the cancer risk factor (CSF) of each individual metal load, the carcinogenic risk (CR) exposure for a lifetime encounter was computed for each pathway. The CSF of metals has been presented in Table 2. When there is more than one carcinogenic pollutant, the risk of developing cancer can be estimated by adding all metals and routes (Wang et al., 2021). Using the following Eqs. (6) and (7), CR and total carcinogenic risk (TCR), can be estimated:

$$CR = CSF \times CDL \quad (6)$$

$$TCR = \sum CR \quad (7)$$

Permissible limits for CR over a lifetime vary from 10^{-6} to 10^{-4} (Yin et al., 2015).

3. Results and discussion

3.1. Trace metal concentration in urban waterway sediment

Trace metal average concentrations (mg/kg) in Kirtankhola River sediment are shown in Table 4, and Fig. 2 demonstrates the spatial distribution of these concentrations. The metal concentration was in the range (mg/kg) of As (1.04–10.07), Pb (0.92–27.67), Hg (0.01–0.64), Fe (4894.93–27,135.65), Mn (60.89–520.33), Cd (0.1–0.6), Cr (3.52–25.22), Cu (0.18–21.86), Ni (2.58–23.46), Zn (12.99–48.40). Sediment quality guidelines (SQGs) have been developed over the years to assist in determining the extent of sediment pollution and its potentially harmful effects on aquatic environments. SQG found that while heavy metal concentrations above the probable effect level (PEL) indicate the possibility of manifold negative impacts, concentrations below the threshold effect level (TEL) are unlikely to have detrimental biological effects (MacDonald et al., 2000; Jolly et al., 2023).

The concentration of metals in the sediment samples from the Kirtankhola River showed an average of As of 6.59 mg/kg. According to SQGs, the TEL value of As (5.9 mg/kg) is less than it. However, the shale value is two-fold higher than the As level. Jolly et al. (2023) also showed As to consist of a higher than average value than the TEL limit. Pb concentrations varied between 0.92 and 27.67 mg/kg, with an average of 8.67 mg/kg. From Table 5, it is observed that the Pb concentration in the Kirtankhola River was below all safety limits and the shale value. Hg

Table 2
Parameters used for human health risk assessment (Non-carcinogenic and Carcinogenic).

Parameter	Unit	Adult		Child	Reference
		Male	Female		
Body Weight (BW)	kg	70	65	15	USEPA (2004)
Exposure Frequency (EF)	days/year	350	350	350	USEPA (2011)
Exposure Duration (ED)	years	30	30	6	USEPA (2011)
Skin surface Area (SA)	cm^2	5700	5700	2800	USEPA (2011)
Adherence Factor (AF)	mg/cm^2	0.07	0.07	0.2	USEPA (2011)
Dermal Absorption factor (ABS)	–	0.001, for As = 0.03	0.001, for As = 0.03	0.001, for As = 0.03	USEPA (2011)
Average Time (AT) for non-carcinogens	days	365 × ED	365 × ED	365 × ED	USEPA (2004)
Average Time (AT) for carcinogens	days	365 × 70	365 × 70	365 × 70	USEPA (2004)
Ingestion Rate (IRS)	mg/day	100	100	200	USEPA (2004)
Inhalation Rate (Inh)	m^3/day	20	20	7.6	USEPA (2004)
Particulate Emission Factor (PEF)	m^3/kg	1.36×10^9	1.36×10^9	1.36×10^9	USEPA (2004)
Carcinogenic Slope Factor (CSF)	mg/kg/d	As = 1.5[a]; Pb = 0.38[b]; Cd = 15[c]; Cr = 0.5[d]; Ni = 1.7[b]			[a] Ferreira-Baptista and De Miguel (2005); [b]Alsafran et al. (2021); [c]Mo et al. (2015); [d] Papillomaviruses (2011)

Table 3
Reference dose (RfD) values for non-carcinogenic risk assessment.

Metal	RfD Dermal (mg/kg/d)	RfD Ingestion (mg/kg/d)	RfD Inhalation (mg/kg/d)	References
As	1.25E-04	3.00E-04	3.01E-04	Ferreira-Baptista and De Miguel (2005)
Pb	5.25E-04	3.50E-03	3.52E-03	Ferreira-Baptista and De Miguel (2005)
Hg	2.10E-05	3.00E-04	8.57E-05	Ferreira-Baptista and De Miguel (2005)
Fe	3.00E-01	3.00E-01	3.00E-01	Zheng et al. (2010)
Mn	1.84E-03	4.60E-02	1.43E-05	Ferreira-Baptista and De Miguel (2005)
Cd	1.00E-03	1.00E-03	1.00E-03	Ferreira-Baptista and De Miguel (2005)
Cr	6.00E-05	3.00E-03	2.86E-03	Ferreira-Baptista and De Miguel (2005)
Cu	1.20E-02	4.00E-02	4.02E-02	Ferreira-Baptista and De Miguel (2005)
Ni	5.40E-03	2.00E-02	2.06E-02	Ferreira-Baptista and De Miguel (2005)
Zn	6.00E-02	3.00E-01	0.30E-01	Ferreira-Baptista and De Miguel (2005)

averaged in concentration at 0.37 mg/kg and is higher than the TEL; however, it is within the standard limits (PEL, SEL, and shale value). The quantities of iron (Fe) in the sediment samples fell within the shale value range, ranging from 4894.93 to 27,135.65 mg/kg and on average 19,330.6 mg/kg. SQGs did not recommend any limit values for Fe and Mn. The concentration of Fe peaked in samples collected from S14 and the lowest concentrations in S5. Mn levels were measured in mg/kg, with a mean of 337.36 and a range of 60.89 to 520.33 mg/kg. The Mn content in the Kirtankhola River was found to be lower than the shale value, as shown in Table 5. Jolly et al. (2023) reported 583.90 mg/kg of Mn in Shitalakshya river sediments, which is nearly twice as high as the current findings. The average concentration of Cd in the study site is 0.37 mg/kg, as shown in Table 5, which is significantly less than the sediment of the Shitalakhya River (Jolly et al., 2023) and Buriganga River (Islam et al., 2018a). These investigations showed a higher concentration because of the continuous industrial activity onshore. The cadmium (Cd) concentration is under SQG safety guidelines but exceeds the shale value (Table 5). The concentration of Cr in Kirtankhola River sediment is 15.50 mg/kg, which is significantly lower than all legislative values (TEL, PEL, SEL, and shale value). According to Islam et al. (2018a), Cr has a value of about twenty-fold greater than the present study, due to the Buriganga being contaminated by the spillage of Cr from the adjacent tannery industries (Jolly et al., 2023). The concentration of Cu varied from 0.18 to 21.86 mg/kg, with a mean value of 12.16 mg/kg, which is lower than the TEL, PEL, SRL, and shale value limits. In the study of Jolly et al. (2023) the concentration of Cu in sediments from the Shitalakshya River was higher, which could be attributed to the release of raw wastewater from surrounding industries. Ni levels ranged between 2.58 and 23.46 mg/kg, with a mean of 14.2 mg/kg. When compared to the Ni levels in the Buriganga (Islam et al., 2018a), the Kirtankhola river sediment displayed lesser values (Table 5). In addition, the Ni concentration is lower than the shale, TEL, PEL, and SEL values. The Zn concentration is 4 times lower than that of the Shitalakhya River, with an average of 35.71 mg/kg (Jolly et al., 2023) and two-fold lower than the South Yellow Sea (Lu et al., 2017) sediment. The Zn concentration in all sampling stations ranges between 12.99 and 48.40 mg/kg, which is lower than all safety limits. S11 showed the highest value of Zn because of fertilizers and industrial wastes. Mirza et al. (2019) obtained almost similar values for Pb (10.30 mg/kg) and Cu (15.63 mg/kg) in the Strait of Khuran (Persian Gulf), Iran.

The following sequence represents the current study's average trace metal concentration: Fe > Mn > Zn > Cr > Ni > Cu > Pb > As > Hg > Cd. Peak concentrations of heavy metals were observed at S11, followed by S12, S15, and S10 stations. This suggested that the contamination of surface sediment with trace metals was caused by the river's downstream flow and the quick rise in urbanization activities (Li et al., 2012). The primary contributors to elevated metal input at S11 and S12 are urban activities such as industrial discharges, municipal waste, and urban runoff.

3.2. *Assessment of geochemical approaches*

An estimate of the trace metal contamination in the study area is provided by the contamination factor (CF). The ratio of each element's concentration in the sediment to its background or baseline is used to calculate it. The current study assessed the CF value for the metal and presented it in Table 6 and Fig. 3(a). The range of the CF for As, Pb, Hg, Fe, Mn, Cd, Cr, Cu, Ni, and Zn is 0.08–0.77, 0.05–0.64, 0.23–1.60, 0.10–0.57, 0.07–0.61, 0.33–2.00, 0.04–0.28, 0.06–0.52, 0.003–0.32, and 0.14–0.51, respectively. Most of the metals showed lower values for contamination factors except for Hg and Cd. Cd showed the highest value with moderate contamination. Based on CF values, Sungur and Özcan (2015) stated that Cr, Pb, Cu, and Ni had moderate contamination status, and Cd showed high contamination in the Kavak delta, Turkey. Islam et al. (2018a) also showed high contamination status for Pb and Cd, with the highest values of 166 and 52, respectively, in the Buriganga

Table 4
Heavy metal concentration (mg/kg) in sediment.

Stations	Heavy metal concentration (mg/kg)									
	As	Pb	Hg	Fe	Mn	Cd	Cr	Cu	Ni	Zn
S – 1	4.54	5.04	0.12	16,599	265.76	0.31	9.80	6.41	9.58	28.48
S – 2	4.92	5.32	0.18	14,666	227.19	0.28	9.33	5.67	8.92	25.97
S – 3	7.49	8.62	0.33	19,046	321.01	0.41	14.05	10.57	13.29	36.04
S – 4	8.14	27.67	0.53	23,473	384.33	0.42	19.96	16.45	19.08	44.30
S – 5	1.04	0.92	0.09	4895	60.89	0.09	3.52	0.18	2.58	12.99
S – 6	6.32	6.13	0.44	20,109	355.66	0.39	15.86	12.77	15.07	38.08
S – 7	4.4	3.12	0.13	11,484	165.42	0.18	9.94	5.95	9.04	26.41
S – 8	5.03	5.19	0.23	14,797	236.27	0.32	11.57	6.58	10.77	30.24
S – 9	4.67	6.00	0.10	15,172	204.82	0.31	9.63	6.26	8.17	27.71
S – 10	8.34	9.43	0.54	23,803	453.45	0.50	21.02	17.32	20.44	43.02
S – 11	10.07	12.86	0.64	25,762	513.47	0.61	25.22	21.86	23.46	48.40
S – 12	9.84	12.06	0.6	25,414	520.33	0.49	22.69	21.32	22.34	46.90
S – 13	7.78	8.06	0.47	23,135	401.41	0.42	19.01	15.55	18.31	40.60
S – 14	8.85	12.47	0.57	27,136	509.16	0.48	22.49	19.93	21.35	44.59
S – 15	7.49	7.10	0.54	24,469	441.17	0.41	18.36	15.58	18.40	41.92
Mean	6.59	8.67	0.37	19,331	337.36	0.37	15.50	12.16	14.20	35.71
SD	2.46	6.26	0.21	6297	140.46	0.13	6.34	6.72	6.31	10.02

River during the winter. The main sources of cadmium are the discharge of municipal waste and the usage of phosphate fertilizers in the agricultural fields adjacent to the river (Islam et al., 2018a).

The pollution load index (PLI) can be employed to compare the pollution status of the study locations. A PLI value below 1 indicates that the sediment is unpolluted, and above this, it denotes existing pollution. The PLI value presented in Table 6 and Fig. 3(b) and the sequence of stations when considering metal enrichment were: S11 > S12 > S14 > S4 > S10 > S15 > S13 > S6 > S3 > S8 > S1 > S2 > S9 > S7 > S5. Sungur and Özcan (2015) revealed that the Kavak delta's mean PLI value was 1.62, indicating metal pollution at the study site.

The geo-accumulation (Igeo) index, which can be calculated using the formula shown in Table 2, is widely utilized to evaluate the degree of trace metal contamination of sediment. The I_{geo} value for each individual element is shown in Fig. 4. The mean I_{geo} value ranged from −3.54 to −0.38, with Ni and Cd representing the minimum and maximum values, respectively (Table 7). All of these falls in class zero, indicating the sediment is unpolluted by trace metals. Mirza et al. (2019) also showed that values for most of the elements Cu, Zn, Cd, Ni, V, and Cr were below zero, signaling a minimal risk of pollution in the investigated area. According to Lu et al. (2017), the I_{geo} values of metals in the northern East China Sea and South Yellow Sea suggested no contamination or minor to moderate pollution in the spring but a higher degree of pollution in the autumn, particularly regarding Pb.

A useful method for assessing the degree of anthropogenic contamination by trace metals is the enrichment factor (EF). Sediments at Kirtankhola displayed a variety of metal enrichment, as seen in Table 8 and Fig. 5. Even though S11 exhibited moderate enrichment for Cd with the highest value (3.66), the mean value of Cd (3.04) showed nearly no enrichment. Apart from Cd, there was no enrichment evident in the mean values of the other metals. The mean EF values of these metals were as follows: Cd > Hg > As> Fe > Pb > Zn > Mn > Cu > Cr > Ni. In a comparable manner, Ghrefat et al. (2011) found that among all the metals Cd had the highest EF in the sediment samples of the Kafrain Dam, Jordan. Among all sites, S11 has the highest EF value and showed moderate enrichment with As, Pb, Hg, and Cd. The Hindon River investigation by Chabukdhara and Nema (2012) detected extremely high levels of Cd and Pb enrichment. Finally, it can be said that none of the stations were completely devoid of anthropogenic enrichment.

The potential ecological risk index (RI) allows for a more accurate assessment of trace metal contamination by combining toxicology with environmental and ecological consequences (Ke et al., 2015). The potential ecological risk index for each metal or for a combination of those was analyzed following the formula shown in Table 1. The hierarchy of E_r^i is Cd > Hg > As >Pb > Cu > Ni > Zn > Cr. While Cd (10–60) had the highest mean single potential ecological risk factor, Hg had the highest value in S11 (64). The risk factor of As, Pb, Cr, Cu, Ni, and Zn was below 40 in all sampling stations, reflecting that these metals pose very little ecological threat (Table 9). According to Rani et al. (2021), Pb, Cr, Cu, and Zn also displayed low potential ecological risk throughout all study sites, whereas a result of indiscriminate disposal of waste from industrial operations in surface waters of Bangladesh, Cd (45–312) exhibited moderate to high ecological risk. In regards to the risk index (RI), the following stations were ranked: S11 > S12 > S14 > S10 > S4 > S15 > S13 > S6 > S3 > S8 > S2 > S1 > S9 > S7 > S5. In accordance with the criterion, stations in the research vicinity had RI ranging between 20.54 and 140.25 (RI < 150), implicating a low pollution level (Fig. 6).

Based on the geochemical approach to pollution assessment, it was found that S11 (Jamuna oil depot) has the highest accumulation of metals, and this could be a consequence of either point or non-point sources (Chabukdhara and Nema, 2012).

3.3. *Chemometric analyses*

3.3.1. *Pearson correlation*

Pearson correlation is a great tool employed to assess the correlation between the source and distribution patterns of metals and the values from the correlation may be positive or negative (Ali et al., 2022a). The strong and moderate correlation between elements suggests that they have similar origins, particularly from point and non-point sources (Hossain et al., 2022). Even a single factor cannot control the metals if there is no correlation between the elements (Külkrer et al., 2014). A significant positive correlation can be seen in the correlation matrix between Cr vs. Cu (0.960), Cu vs. Mn (0.948), Cu vs. Fe (0.945), Fe vs. Mn (0.936), Hg vs. Cu (0.930), Cu vs. Ni (0.929), and Cr vs. Zn (0.928), with a confidence level of 99 % ($p < 0.01$ significance) (Table 10). This correlation suggests that they most likely have similar origins and that they may share a common anthropogenic source, such as industrial effluents, municipal waste, oil refineries, and inputs from agriculture.

3.3.2. *Principal component analysis (PCA)*

Principal component analysis (PCA), which is considered a dependable method for identifying sources, was employed to determine potential sources of trace metals in sediment from various sites along the Kirtankhola River (Islam et al., 2018a).

From the scree plot, 10 principal components have been generated (Comp.1 to Comp.10), which also correspond to the number of variables in the data (Fig. 7a). Each component of the PCA explains a percentage of the total variance found within the data set. The first principal component explains almost 79.69 % of the total variance. This implies

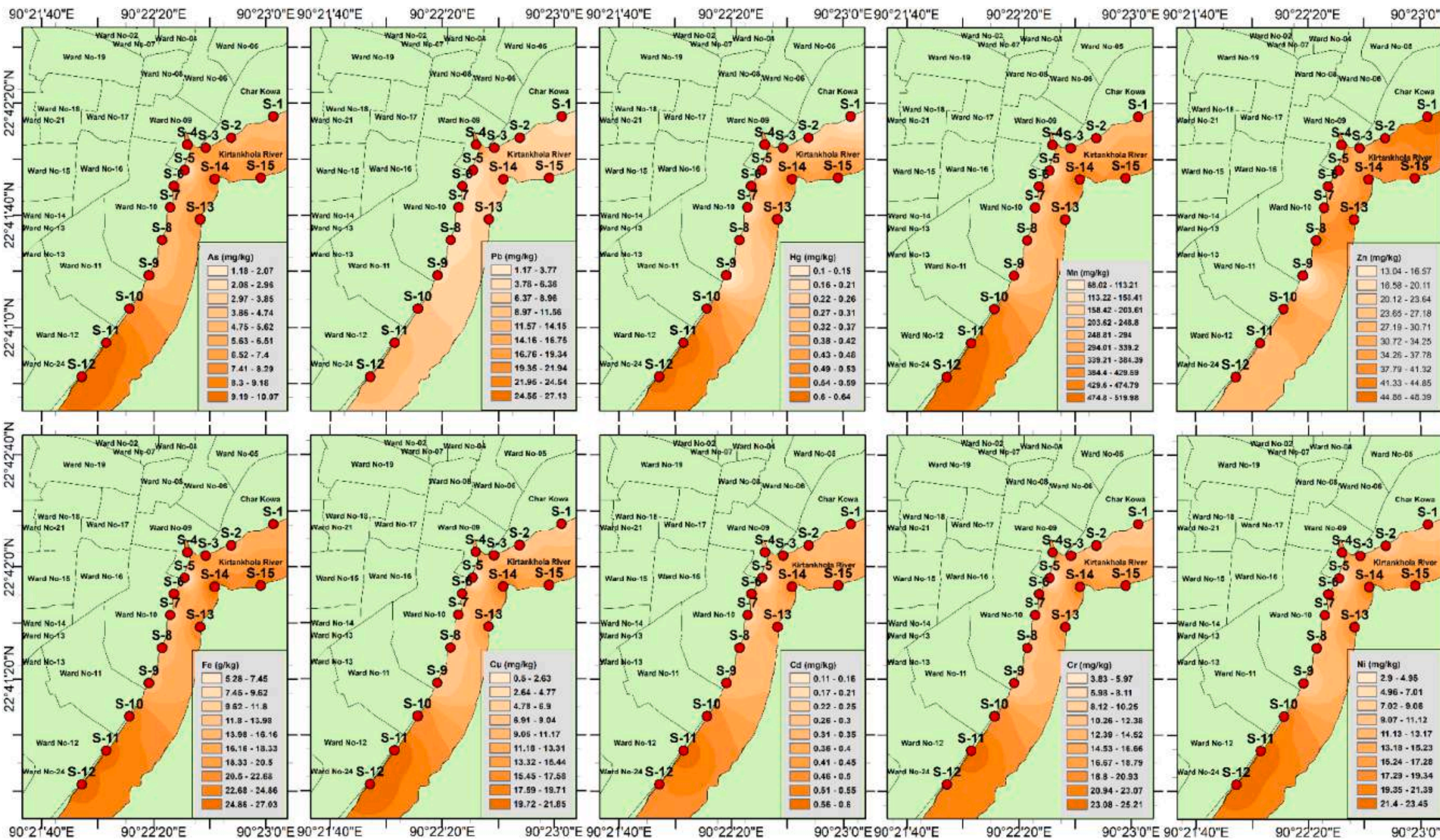

Fig. 2. Spatial distribution of the trace metals in surface sediments of river.

Table 5
Comparison of metals in sediment (mg/kg) with some reported and reference values.

Sampling area	Metal concentration (mg/kg)										References
	As	Pb	Hg	Fe	Mn	Cd	Cr	Cu	Ni	Zn	
Kirtankhola, Bangladesh	6.59	8.67	0.37	19,331	337.36	0.37	15.50	12.16	14.2	35.71	Present study
Shitalakhya, Bangladesh	13.65	19.80	–	–	583.90	4.88	68.14	143.87	37.27	157.85	Jolly et al. (2023)
Buriganga, Bangladesh	21	731	–	–	–	7.7	297	280	240	–	Islam et al. (2018a)
Strait of Khuran (Persian Gulf), Iran	–	10.30	–	2230	–	0.14	102.40	15.63	89.37	40.94	Mirza et al. (2019)
South Yellow Sea and northern East China Sea	–	23.3	–	–	–	–	72.3	21.4	32.4	77.9	Lu et al. (2017)
TEL	5.9	35	0.174	–	–	0.596	37.3	35.7	18	123	MacDonald et al. (2000)
PEL	17	91.3	0.486	–	–	3.53	90	197	36	315	MacDonald et al. (2000)
SEL	33	250	2	–	–	10	110	110	75	820	MacDonald et al. (2000)
Shale value	13	20	0.4	47,200	850	0.3	90	45	68	95	Turekian and Wedepohl (1961)

TEL = Threshold effect level; PEL = Probable effect level; SEL = Severe effect level.

Table 6
Contamination factor (CF), Pollution load index (PLI) of trace metals in sediments.

Stations	As	Pb	Hg	Fe	Mn	Cd	Cr	Cu	Ni	Zn	PLI
S – 1	0.35	0.25	0.30	0.35	0.31	1.00	0.11	0.21	0.09	0.30	0.268
S – 2	0.38	0.27	0.45	0.31	0.27	1.00	0.10	0.20	0.08	0.27	0.266
S – 3	0.58	0.43	0.83	0.40	0.38	1.33	0.16	0.30	0.16	0.38	0.403
S – 4	0.63	1.38	1.33	0.50	0.45	1.33	0.22	0.42	0.24	0.47	0.570
S – 5	0.08	0.05	0.23	0.10	0.07	0.33	0.04	0.06	0.003	0.14	0.066
S – 6	0.49	0.31	1.10	0.43	0.42	1.33	0.18	0.33	0.19	0.40	0.421
S – 7	0.34	0.16	0.33	0.24	0.19	0.67	0.11	0.20	0.09	0.28	0.222
S – 8	0.39	0.26	0.58	0.31	0.28	1.00	0.13	0.24	0.10	0.32	0.294
S – 9	0.36	0.30	0.25	0.32	0.24	1.00	0.11	0.18	0.09	0.29	0.253
S – 10	0.64	0.47	1.35	0.50	0.53	1.67	0.23	0.45	0.25	0.45	0.543
S – 11	0.77	0.64	1.60	0.55	0.60	2.00	0.28	0.52	0.32	0.51	0.646
S – 12	0.76	0.60	1.50	0.54	0.61	1.67	0.25	0.50	0.31	0.49	0.611
S – 13	0.60	0.40	1.18	0.49	0.47	1.33	0.21	0.41	0.23	0.43	0.486
S – 14	0.68	0.62	1.43	0.57	0.60	1.67	0.25	0.47	0.29	0.47	0.596
S – 15	0.58	0.36	1.35	0.52	0.52	1.33	0.20	0.41	0.23	0.44	0.492
Mean	0.51	0.43	0.92	0.41	0.40	1.24	0.17	0.33	0.18	0.38	0.409

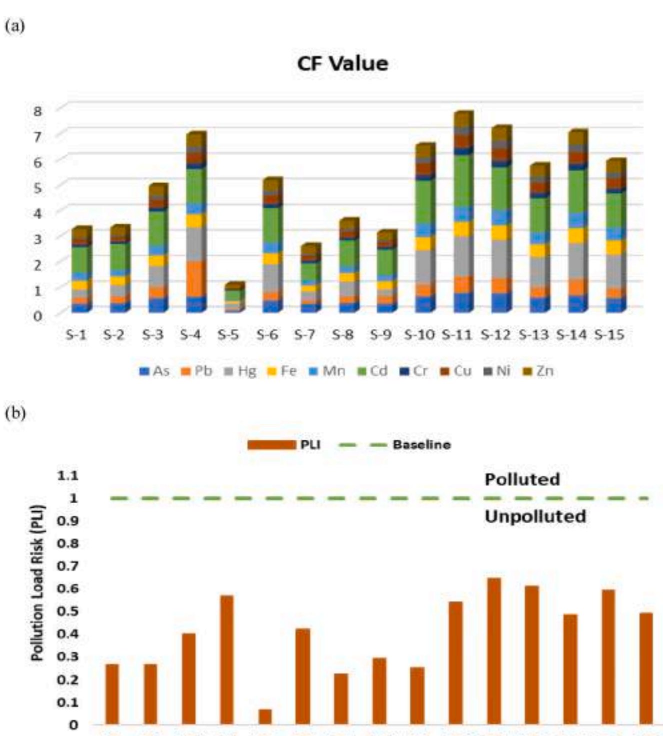

Fig. 3. (a) Contamination Factor (CF); and (b) Pollution Load Index (PLI) of different stations.

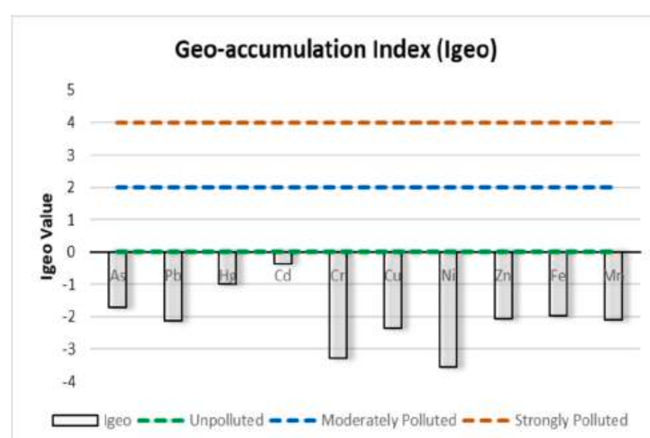

Fig. 4. Geo-accumulation Index (Igeo) of trace metals in different sampling stations of the river sediments.

that almost two-thirds of the data in the set of 10 variables can be represented by just the first principal component. The second component explains 11.79 % of the total variance (Fig. 7b). The cumulative proportion of Comp.1 and Comp.2 explains nearly 91.47 % of the total variance. This indicates that the data can be accurately represented by the first two principal components. The loading matrix shows that the first principal component has high positive values for As, Hg, Cd, Cr, Cu, Ni, Zn, Fe, and Mn. However, the values for Pb are relatively in the negative spectrum. When it comes to the second principal component, it has high negative values for Pb, Hg, Cr, Cu, and Zn (Table 11).

Table 7
Geo-accumulation index (I_{geo}) of trace metals in sediments.

Stations	As	Pb	Hg	Fe	Mn	Cd	Cr	Cu	Ni	Zn
S – 1	−2.10	−2.57	−2.32	−2.09	−2.26	−0.58	−3.78	−2.82	−3.99	−2.32
S – 2	−1.99	−2.50	−1.74	−2.27	−2.49	−0.58	−3.85	−2.92	−4.17	−2.46
S – 3	−1.38	−1.80	−0.86	−1.89	−1.99	−0.17	−3.26	−2.34	−3.27	−1.98
S – 4	−1.26	−0.12	−0.18	−1.59	−1.73	−0.17	−2.76	−1.82	−2.63	−1.69
S – 5	−4.23	−5.03	−2.74	−3.85	−4.39	−2.17	−5.26	−4.71	−9.15	−3.46
S – 6	−1.63	−2.29	−0.45	−1.82	−1.84	−0.17	−3.09	−2.16	−3.00	−1.90
S – 7	−2.15	−3.27	−2.21	−2.62	−2.95	−1.17	−3.76	−2.90	−4.10	−2.43
S – 8	−1.95	−2.53	−1.38	−2.26	−2.43	−0.58	−3.54	−2.65	−3.95	−2.24
S – 9	−2.06	−2.32	−2.58	−2.22	−2.64	−0.58	−3.81	−3.05	−4.03	−2.36
S – 10	−1.23	−1.67	−0.15	−1.57	−1.49	0.15	−2.68	−1.72	−2.56	−1.73
S – 11	−0.95	−1.22	0.09	−1.46	−1.31	0.42	−2.42	−1.52	−2.22	−1.56
S – 12	−0.99	−1.31	0.00	−1.48	−1.29	0.15	−2.57	−1.60	−2.26	−1.60
S – 13	−1.33	−1.90	−0.35	−1.61	−1.67	−0.17	−2.83	−1.88	−2.71	−1.81
S – 14	−1.14	−1.27	−0.07	−1.38	−1.32	0.15	−2.59	−1.66	−2.36	−1.68
S – 15	−1.38	−2.08	−0.15	−1.53	−1.53	−0.17	−2.88	−1.88	−2.71	−1.77
Mean	−1.72	−2.13	−1.01	−1.98	−2.09	−0.38	−3.27	−2.38	−3.54	−2.07

Table 8
Enrichment factor (EF) of trace metals in sediments.

Stations	As	Pb	Hg	Fe	Mn	Cd	Cr	Cu	Ni	Zn
S – 1	0.99	0.72	0.85	1	0.89	2.84	0.31	0.61	0.27	0.85
S – 2	1.22	0.86	1.45	1	0.86	3.22	0.33	0.64	0.27	0.88
S – 3	1.43	1.07	2.04	1	0.94	3.30	0.39	0.73	0.39	0.94
S – 4	1.26	2.78	2.66	1	0.91	2.68	0.45	0.85	0.49	0.94
S – 5	0.77	0.44	2.17	1	0.69	3.21	0.38	0.55	0.03	1.32
S – 6	1.14	0.72	2.58	1	0.98	3.13	0.41	0.79	0.44	0.94
S – 7	1.39	0.64	1.34	1	0.80	2.74	0.45	0.83	0.36	1.14
S – 8	1.23	0.83	1.83	1	0.89	3.19	0.41	0.76	0.31	1.02
S – 9	1.12	0.93	0.78	1	0.75	3.11	0.33	0.56	0.29	0.91
S – 10	1.27	0.93	2.68	1	1.06	3.30	0.46	0.90	0.51	0.90
S – 11	1.42	1.18	2.93	1	1.11	3.66	0.51	0.96	0.59	0.93
S – 12	1.41	1.12	2.79	1	1.14	3.10	0.47	0.92	0.58	0.92
S – 13	1.22	0.82	2.40	1	0.96	2.72	0.43	0.83	0.47	0.87
S – 14	1.18	1.08	2.48	1	1.04	2.90	0.43	0.83	0.51	0.82
S – 15	1.11	0.68	2.60	1	1.00	2.57	0.39	0.79	0.44	0.85
Mean	1.21	0.99	2.11	1	0.93	3.04	0.41	0.77	0.40	0.95

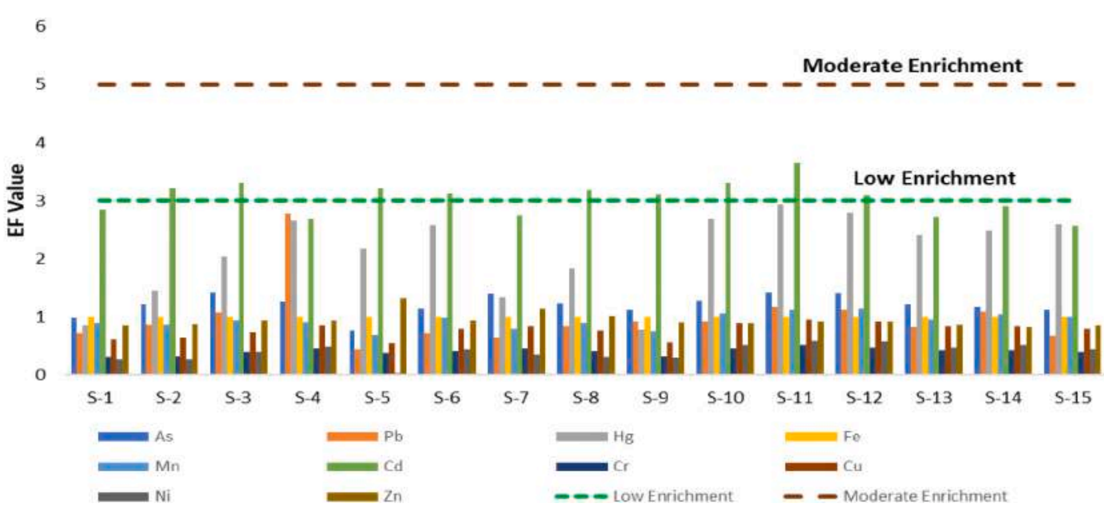

Fig. 5. Enrichment Factor (EF) of trace metals in different sampling stations of the river sediments.

Pb, Mn, Cd and Hg are the top four variables with the highest cos2, hence contributing the most to PC1 and PC2. From the biplot:

- Attributes with high cos2 values are represented in green: Pb, Mn, and Cd.
- Attributes with mid cos2 values are depicted in orange: Hg, Cr and Cu.
- Lastly, attributes with low cos2 values are indicated in black: Zn, As, Fe and Ni.

3.3.3. *Cluster analysis (CA)*

Clustering correlated features together is helpful when dealing with correlations between a large number of features. With the use of variables that demonstrate similarities within the same group and disparities

Table 9
Potential ecological risk factor and Potential ecological risk index (RI) of trace metals in sediments.

Stations	Potential ecological risk factor E_r^i								RI
	As	Pb	Hg	Cd	Cr	Cu	Ni	Zn	
S – 1	3.49	1.26	12	30	0.22	1.06	0.47	0.30	48.81
S – 2	3.78	1.33	18	30	0.21	0.99	0.42	0.27	55.00
S – 3	5.76	2.16	33	40	0.31	1.48	0.78	0.38	83.86
S – 4	6.26	6.92	53	40	0.44	2.12	1.21	0.47	110.42
S – 5	0.8	0.23	9	10	0.08	0.29	0.01	0.14	20.54
S – 6	4.86	1.53	44	40	0.35	1.67	0.94	0.40	93.76
S – 7	3.38	0.78	13	20	0.22	1.00	0.44	0.28	39.11
S – 8	3.87	1.30	23	30	0.26	1.20	0.48	0.32	60.42
S – 9	3.59	1.50	10	30	0.21	0.91	0.46	0.29	46.97
S – 10	6.42	2.36	54	50	0.47	2.27	1.27	0.45	117.24
S – 11	7.75	3.22	64	60	0.56	2.61	1.61	0.51	140.25
S – 12	7.57	3.02	60	50	0.50	2.48	1.57	0.49	125.63
S – 13	5.98	2.02	47	40	0.42	2.03	1.14	0.43	99.03
S – 14	6.81	3.12	57	50	0.50	2.37	1.47	0.47	121.73
S – 15	5.76	1.78	54	40	0.41	2.04	1.15	0.44	105.58
Mean	5.07	2.17	36.73	37.33	0.34	1.64	0.89	0.38	84.56

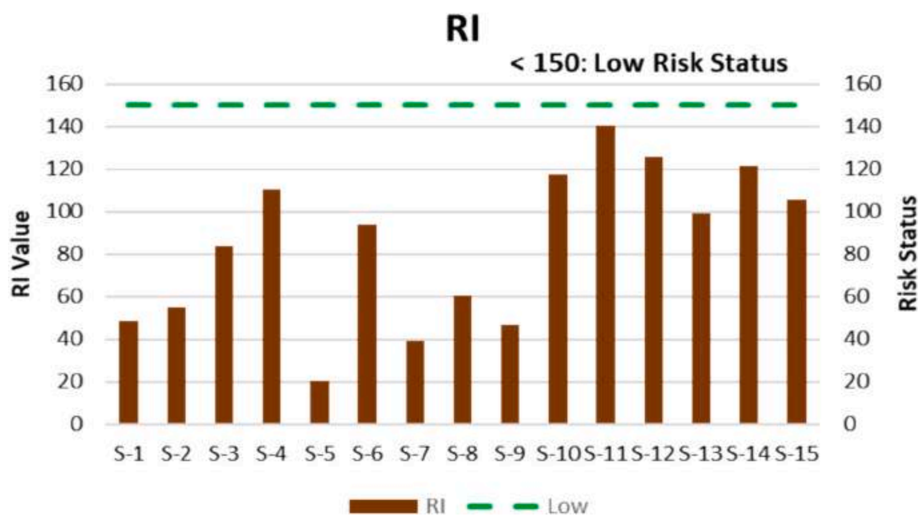

Fig. 6. Potential ecological risk index (RI) of different sampling stations.

Table 10
Pearson correlation matrix of the metals from the study area.

	As	Pb	Hg	Cd	Cr	Cu	Ni	Zn	Fe	Mn
As	1									
Pb	0.615(**)	1								
Hg	0.838(**)	0.615(**)	1							
Cd	0.837(**)	0.563(**)	0.713(**)	1						
Cr	0.864(**)	0.625(**)	0.895(**)	0.803(**)	1					
Cu	0.919(**)	0.636(**)	0.930(**)	0.847(**)	0.960(**)	1				
Ni	0.833(**)	0.629(**)	0.839(**)	0.890(**)	0.903(**)	0.929(**)	1			
Zn	0.888(**)	0.658(**)	0.888(**)	0.790(**)	0.928(**)	0.912(**)	0.883(**)	1		
Fe	0.911(**)	0.636(**)	0.878(**)	0.866(**)	0.903(**)	0.945(**)	0.907(**)	0.907(**)	1	
Mn	0.911(**)	0.544(**)	0.875(**)	0.835(**)	0.879(**)	0.948(**)	0.879(**)	0.877(**)	0.936(**)	1

** Correlation is significant at the 0.01 level (2-tailed).

between various groups, homogenous clusters are created using cluster analysis (CA) and displayed as a dendrogram. In order to establish a relationship between the metal concentration and its potential source, the cluster map function groups pertinent features using hierarchical clustering to create dendrograms that resemble trees.

There are notable clusters in this plot (Fig. 8). The blue cluster, which is closest to the origin, contains the individuals with the best results, while the red contains individuals with the worst results. Pb, which makes up Cluster 1, may have come from engine exhaust and oil that leaks into water bodies from boats and steamers (Jolly et al., 2023). Besides, As, Cd, Cr, Fe, Mn, Cu, Hg, Ni, and Zn were confined to cluster 2 and may either be attributed to natural processes (rock and soil weathering, etc.) or anthropogenic activities e.g. chemical and other industries, oil refineries, industrial effluents, household wastes and agricultural activities. Previous studies discovered that chemical fertilizers and herbicides applied to farmland, among other agricultural practices, raised the concentrations of Cu and Zn in sediment (Islam et al., 2023; Rani et al., 2021). Warehouse and metal industries

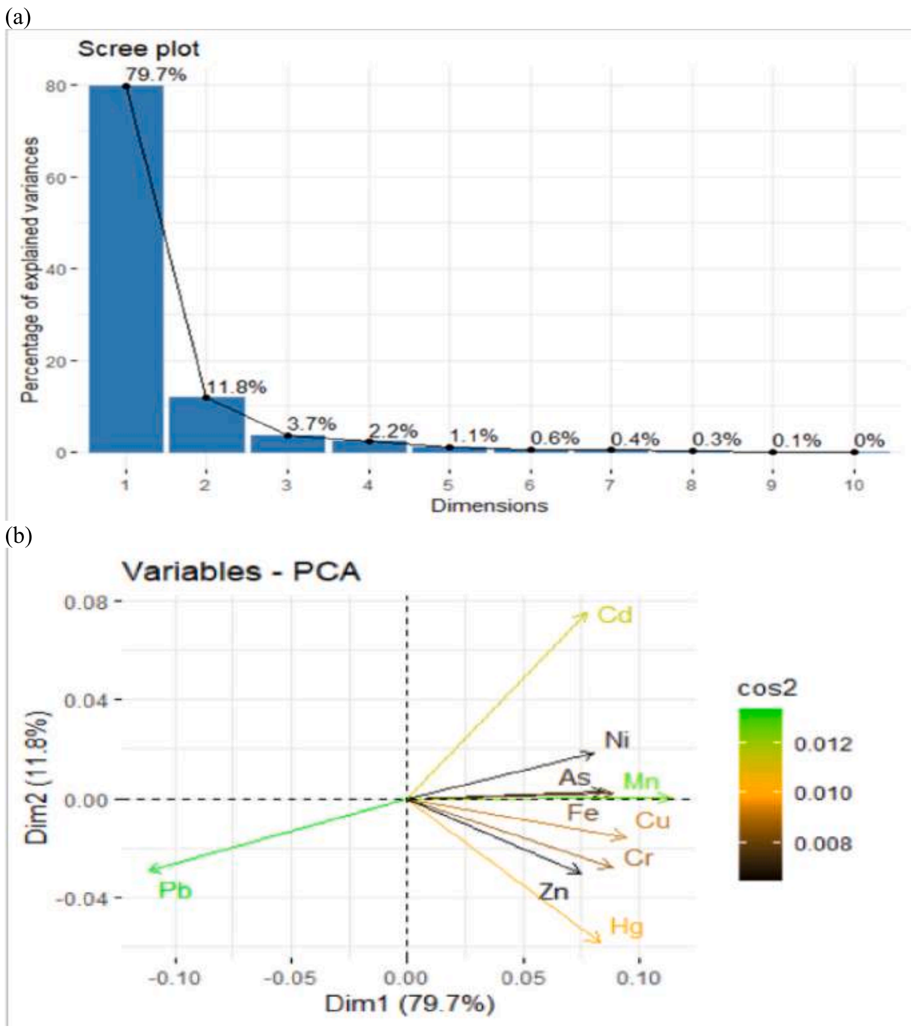

Fig. 7. (a) Scree plot and (b) variable PCA plot for trace metals.

Table 11
Loading matrix of the first two principal components.

	Comp.1	Comp.2
As	0.2965225	0.024055462
Pb	−0.3892931	−0.266341407
Hg	0.2885505	−0.527921932
Cd	0.2704555	0.680941549
Cr	0.3089961	−0.252445141
Cu	0.3284293	−0.141147953
Ni	0.2820242	0.166028585
Zn	0.2619764	−0.273024417
Fe	0.3089903	0.018387610
Mn	0.3963951	0.001846228

contributed As, Cu, and Zn, while Cd and Ni loads came from the fuel oil and refinery industries. Ferry terminals and cargo ports are likely the main sources of Mn and Zn.

3.4. Assessment of human health risk

Table 12 shows the estimated non-carcinogenic risk of the trace metals As, Hg, Pb, Cd, Cr, Cu, Ni, Zn, Mn, and Fe in the sediment of the Kirtankhola River for both adults and children. For adults (both male and female), the HQ value for individual route dermal came out to be As> Cr > Mn > Fe > Hg > Pb > Ni > Cu > Zn > Cd, with a similar tendency for children. Added to that, the sequence of occurrence was Fe > As >Mn > Cr > Pb > Hg > Ni > Cd > Cu > Zn via ingestion and Mn > Fe > As > Cr > Hg > Pb > Zn > Ni > Cd > Cu via inhalation for both males and females, with comparable findings in children. People are most exposed to As, Fe, Mn, and Cr of all the heavy metals studied. Children have a higher HQ value and seem to be more vulnerable than adults. Fe showed a higher value through the ingestion route for all groups, particularly for children (8.24E-01), almost crossing the threshold value. However, all of the estimated HQ values did not exceed the upper level for the specific route of exposure, proving no health concern. The average HI values were as follows: child > adult female > adult male (Table 13 and Fig. 9). Li et al. (2014) discovered a similar conclusion, as did Ma et al. (2018), who reported the HI value hierarchy is child (1.92) > female (1.68) > male (1.50). Children are more prone to environmental pollutants because of their elevated rate of respiration per body weight, soil-to-mouth processes, and greater gastrointestinal uptake of certain hazardous elements (Li et al., 2014). This finding coincided with prior research, which found that children posed a substantially higher non-carcinogenic risk (Jolly et al., 2023).

Carcinogenic risks for As, Pb, Cd, Cr, and Ni are assessed among the trace metals. Table 14 shows the estimated results of this investigation, which computed the carcinogenic risk for both, adult males and females, along with children. The findings revealed that the CR for all groups of people is within the threshold limit of 1×10^{-6} to 1×10^{-4}. Nickel had a greater value for the ingestion route, while dermal absorption is the prominent approach for As. Pb, Hg, and Cd showed cancer risk values within 1.00E-05 for all groups of people, whereas As and Ni did not

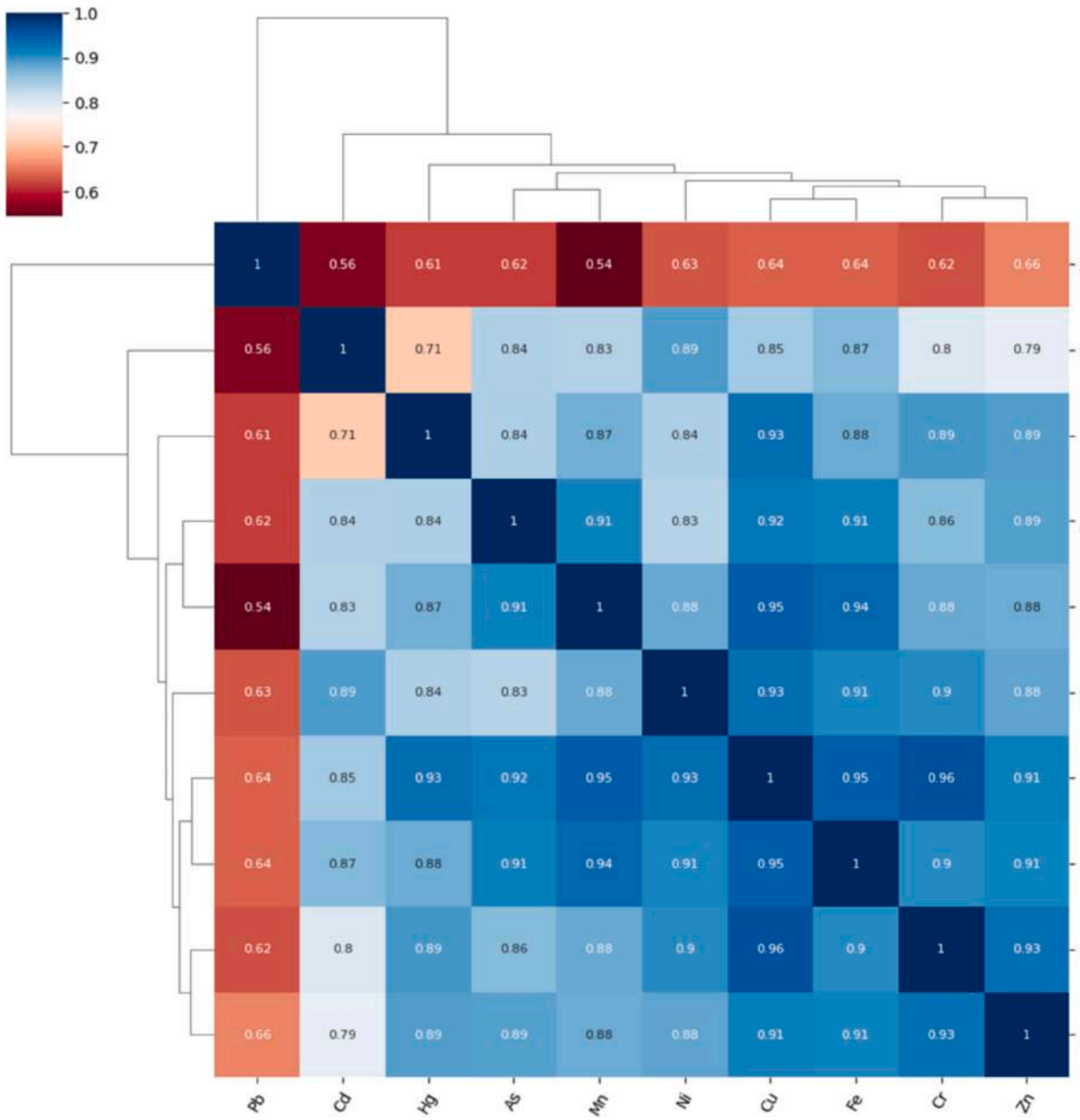

Fig. 8. Hierarchical cluster analysis (dendrogram) of the variables in the study area.

Table 12
Non-carcinogenic risk (HQ) values for individual pathways (Dermal, Ingestion, and Inhalation).

Metals	Male			Female			Child		
	HQ Dermal	HQ Ingestion	HQ Inhalation	HQ Dermal	HQ Ingestion	HQ Inhalation	HQ Dermal	HQ Ingestion	HQ Inhalation
As	8.65E-03	3.01E-02	4.41E-06	9.32E-03	3.24E-02	4.75E-06	5.67E-02	2.81E-01	7.83E-06
Pb	9.02E-05	3.39E-03	4.96E-07	9.72E-05	3.65E-03	5.34E-07	5.91E-04	3.17E-02	8.79E-07
Hg	9.56E-05	1.68E-03	8.63E-07	1.03E-04	1.81E-03	9.30E-07	6.26E-04	1.57E-02	1.53E-06
Fe	3.52E-04	8.83E-02	1.30E-05	3.79E-04	9.51E-02	1.40E-05	2.31E-03	8.24E-01	2.30E-05
Mn	1.00E-03	1.00E-02	4.75E-03	1.08E-03	1.08E-02	5.12E-03	6.56E-03	9.38E-02	8.43E-03
Cd	2.04E-06	5.11E-04	7.52E-08	2.2E-06	5.51E-04	8.10E-08	1.34E-05	4.77E-03	1.33E-07
Cr	1.41E-03	7.08E-03	1.09E-06	1.52E-03	7.62E-03	1.18E-06	9.25E-03	6.60E-02	1.94E-06
Cu	5.54E-06	4.16E-04	6.09E-08	5.96E-06	4.48E-04	6.56E-08	3.63E-05	3.89E-03	1.08E-07
Ni	1.49E-05	1.01E-03	1.44E-07	1.60E-05	1.09E-03	1.55E-07	9.76E-05	9.41E-03	2.55E-07
Zn	3.25E-06	1.63E-04	2.40E-07	3.50E-06	1.76E-04	2.58E-07	2.13E-05	1.52E-03	4.25E-07

Table 13
Hazard Index (HI) and Total Carcinogenic Risk (TCR) values of trace metals.

Metals	Male		Female		Child	
	Hazard Index (HI)	Total Carcinogenic Risk (TCR)	Hazard Index (HI)	Total Carcinogenic Risk (TCR)	Hazard Index (HI)	Total Carcinogenic Risk (TCR)
As	3.88E-02	1.52E-05	4.17E-02	1.63E-05	3.38E-01	1.37E-04
Pb	3.48E-03	4.53E-06	3.75E-03	4.88E-06	3.22E-02	4.22E-05
Hg	1.77E-03	–	1.91E-03	–	1.63E-02	–
Fe	8.86E-02	–	9.55E-02	–	8.26E-01	–
Mn	1.58E-02	–	1.70E-02	–	1.09E-01	–
Cd	5.14E-04	7.70E-06	5.53E-04	8.30E-06	4.79E-03	7.18E-05
Cr	8.49E-03	1.07E-05	9.14E-03	1.15E-05	7.53E-02	9.93E-05
Cu	4.22E-04	–	4.55E-04	–	3.92E-03	–
Ni	1.02E-03	3.44E-05	1.10E-03	3.71E-05	9.51E-03	3.21E-04
Zn	1.67E-04	–	1.79E-04	–	1.54E-03	–
Mean	1.59E-02	1.45E-05	1.71E-02	1.56E-05	1.42E-01	1.34E-04

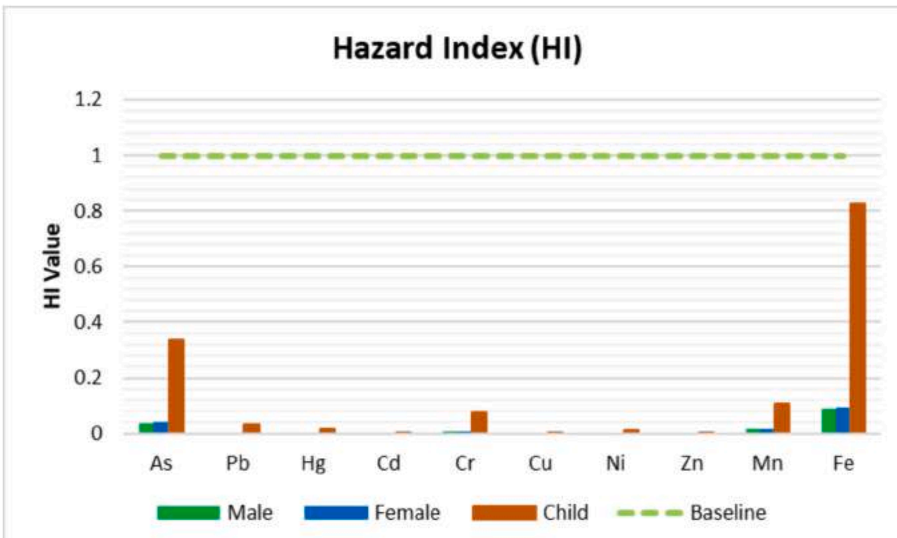

Fig. 9. Hazard Index (HI) value of male, female, and child.

Table 14
Carcinogenic risk (CR) values for individual pathways (Dermal, Ingestion, and Inhalation).

Metals	Male			Female			Child		
	CR Dermal	CR Ingestion	CR Inhalation	CR Dermal	CR Ingestion	CR Inhalation	CR Dermal	CR Ingestion	CR Inhalation
As	1.62E-06	1.36E-05	1.99E-09	1.75E-06	1.46E-05	2.15E-09	1.06E-05	1.26E-04	3.53E-09
Pb	1.80E-08	4.51E-06	6.63E-10	1.94E-08	4.86E-06	7.14E-10	1.18E-07	4.21E-05	1.18E-09
Cd	3.06E-08	7.67E-06	1.13E-09	3.30E-08	8.26E-06	1.21E-09	2.00E-07	7.16E-05	2.00E-09
Cr	4.24E-08	1.06E-05	1.56E-09	4.56E-08	1.14E-05	1.68E-09	2.77E-07	9.91E-05	2.77E-09
Ni	1.37E-07	3.43E-05	5.04E-09	1.47E-07	3.69E-05	5.43E-09	8.96E-07	3.20E-04	8.94E-09

follow this trend. The extent of carcinogenic threat through the ingestion route was reported to be 1.26E-04 and 3.20E-04 for children in As and Ni, respectively, indicating medium risk to children. Jolly et al. (2023) discovered a similar conclusion, reporting that As had a higher carcinogenic risk value for children via ingestion. The ingestion route produced a substantially greater value, indicating that humans are more vulnerable to it as biomagnified heavy metals are consumed by humans through the food web (i.e., fish). For children, the total carcinogenic risk (TCR) of every single metal was organized in the following descending trend: Ni (3.21E-04) > As (1.37E-04) > Cr (9.93E-05) > Cd (7.18E-05) > Pb (4.22E-05), the adult group (both male and female) followed the same trend (Fig. 10). Ma et al. (2018) also reported that humans were significantly vulnerable to Ni, primarily from natural sources, which is the key factor causing carcinogenic risks. Total carcinogenic risk readings for males, females, and children were 1.45E-05, 1.56E-05, and 1.34E-04, respectively (Table 13), demonstrating children had a comparatively higher risk than adults. However, it can be concluded that the Kirtankhola River sediment will pose no cancer risk to the population.

4. Limitations

The study's analyzed locations might not entirely reflect Kirtankhola's total environmental condition. Additionally, selecting exposure criteria is critical in assessing human health risks. The human body exposure parameters and the trace metal toxicity parameters were drawn mostly following USEPA recommendations as well as worldwide study outcomes to reduce the possibility of inaccuracy. However, the dubious effects introduced by these exposure parameters cannot be totally eliminated.

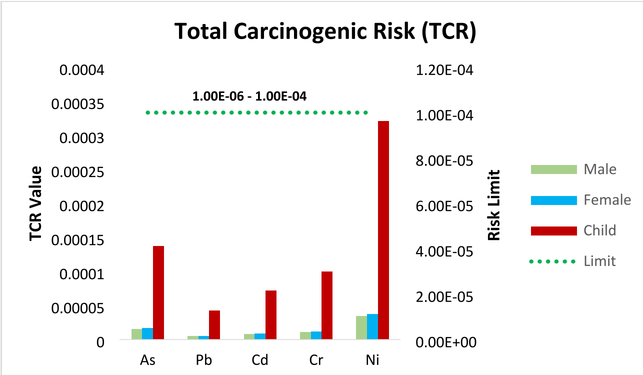

Fig. 10. Total carcinogenic risk (TCR) of male, female, and child.

5. Conclusion

This study investigated the trace metal contents in sediments from upstream and downstream of an urban waterway. Concerns were raised about the contamination of Cd among those metals, especially in sediments originating downstream. It should be noted that S11 and S12 had a higher value than those in the others since they were located downstream of the river and received metal loading from upstream. Considering that char is produced by the deposition of large amounts of sediment, samples from char Kauwa (S13, S14, and S15) had much higher levels of metals, suggesting that the sediment is polluted by untreated residential and agricultural waste. The geo-accumulation index for every metal across all sampling stations showed a negative value, indicating that the sediments are almost unpolluted by these metals. Except for Hg and Cd, all metals in all locations posed a minimal ecological risk. The risk of developing non-carcinogenic health effects was within the acceptable range. The predicted CR value revealed no carcinogenic risk for each group of people. On the contrary, the TCR of children showed a value that was close to violating the safe limit; therefore, particular precautions should be taken and regular monitoring is advised.

Funding

This research was done under the Research and Development (R&D) project, which is funded by the Bangladesh Council of Scientific and Industrial Research (BCSIR) and partially funded by the Ministry of Science and Technology, People's Republic of Bangladesh under the special research grant (project id-SRG -233446 and FY 2023-24).

CRediT authorship contribution statement

Md Kamal Hossain: Writing – review & editing, Supervision, Funding acquisition, Formal analysis, Data curation, Conceptualization. **Fahima Islam:** Writing – original draft, Data curation. **Kowshik Das Karmaker:** Writing – review & editing, Methodology. **Umme Sarmeen Akhtar:** Formal analysis. **Afroza Parvin:** Formal analysis, Data curation. **Mohammad Moniruzzaman:** Resources. **Badhan Saha:** Formal analysis. **Priyanka Dey Suchi:** Resources. **Md Anwar Hossain:** Software, Formal analysis. **Md Aftab Ali Shaikh:** Writing – review & editing, Writing – original draft, Conceptualization.

Declaration of competing interest

According to the authors, there are no known conflicting financial interests or personal connections that might appear to have impacted the findings revealed in this study.

Data availability

Data will be made available on request.

Appendix A. Supplementary data

Supplementary data to this article can be found online at https://doi.org/10.1016/j.marpolbul.2024.116483.

References

Akter, S., Ahmed, K.R., Marandi, A., Schüth, C., 2020. Possible factors for increasing water salinity in an embanked coastal island in the Southwest Bengal Delta of Bangladesh. Sci. Total Environ. 713, 136668 https://doi.org/10.1016/j.scitotenv.2020.136668.

Ali, M.M., Ali, M.L., Islam, M.S., Rahman, M.Z., 2016. Preliminary assessment of heavy metals in water and sediment of Karnaphuli River, Bangladesh. Environ. Nanotechnol. Monit. Manag. 5, 27–35. https://doi.org/10.1016/j.enmm.2016.01.002.

Ali, M.M., Ali, M.L., Rakib, M.R.J., Islam, M.S., Bhuyan, M.S., Senapathi, V., Chung, S.Y., Roy, P.D., Sekar, S., Islam, A.R.M.T., Rahman, M.Z., 2022a. Seasonal behavior and accumulation of some toxic metals in commercial fishes from Kirtankhola tidal river of Bangladesh–a health risk taxation. Chemosphere 301, 134660. https://doi.org/10.1016/j.chemosphere.2022.134660.

Ali, M.M., Rahman, S., Islam, M.S., Rakib, M.R.J., Hossen, S., Rahman, M.Z., 2022b. Distribution of heavy metals in water and sediment of an urban river in a developing country: a probabilistic risk assessment. Int. J. Sediment Res. 37 (2), 173–187. https://doi.org/10.1016/j.ijsrc.2021.09.002.

Alsafran, M., Usman, K., Rizwan, M., Ahmed, T., Al Jabri, H., 2021. The carcinogenic and non-carcinogenic health risks of metal (oid) s bioaccumulation in leafy vegetables: a consumption advisory. Front. Environ. Sci. 9, 380. https://doi.org/10.3389/fenvs.2021.742269.

Bai, J.H., Xiao, R., Zhang, K.J., Gao, H.F., 2012. Arsenic and heavy metal pollution in wetland soils from tidal freshwater and salt marshes before and after the flow-sediment regulation regime in the Yellow River Delta China. J. Hydrol. 450–451, 244–253. https://doi.org/10.1016/j.jhydrol.2012.05.006.

Bhuyan, M.S., Bakar, M.A., Akhtar, A., Hossain, M.B., Ali, M.M., Islam, M.S., 2017. Heavy metal contamination in surface water and sediment of the Meghna River, Bangladesh. Environ. Nanotechnol. Monit. Manag. 8, 273–279. https://doi.org/10.1016/j.enmm.2017.10.003.

Birch, G.F., Olmos, M.A., 2008. Sediment-bound heavy metals as indicators of human influence and biological risk in coastal water bodies. ICES J. Mar. Sci. 65 (8), 1407–1413. https://doi.org/10.1093/icesjms/fsn139.

Brereton, R.G., 1990. Chemometrics: Applications of Mathematics and Statistics to Laboratory Systems. Ellis Horwood, Chichester.

Chabukdhara, M., Nema, A.K., 2012. Assessment of heavy metal contamination in Hindon River sediments: a chemometric and geochemical approach. Chemosphere 87 (8), 945–953. https://doi.org/10.1016/j.chemosphere.2012.01.055.

Ferreira-Baptista, L., De Miguel, E., 2005. Geochemistry and risk assessment of street dust in Luanda, Angola: a tropical urban environment. Atmos. Environ. 39 (25), 4501–4512. https://doi.org/10.1016/j.atmosenv.2005.03.026.

Ghrefat, H., Yusuf, N., 2006. Assessing Mn, Fe, cu, Zn, and cd pollution in bottom sediments of Wadi Al-Arab Dam, Jordan. Chemosphere 65 (11), 2114–2121. https://doi.org/10.1016/j.chemosphere.2006.06.043.

Ghrefat, H.A., Abu-Rukah, Y., Rosen, M.A., 2011. Application of geoaccumulation index and enrichment factor for assessing metal contamination in the sediments of Kafrain Dam, Jordan. Environ. Monit. Assess. 178, 95–109. https://doi.org/10.1007/s10661-010-1675-1.

Hakanson, L., 1980. An ecological risk index for aquatic pollution control. A sedimentological approach. Water Res. 14 (8), 975–1001. https://doi.org/10.1016/0043-1354(80)90143-8.

Hossain, H.M.Z., 2022. Spatial distribution and pollution assessment of heavy metals in sediments from the Brahmaputra River watershed in Bangladesh. Environ. Sci. Pollut. Res. 29, 81557–81570. https://doi.org/10.1007/s11356-022-21522-1.

Hossain, M.B., Runu, U.H., Sarker, M.M., Hossain, M.K., Parvin, A., 2021. Vertical distribution and contamination assessment of heavy metals in sediment cores of ship breaking area of Bangladesh. Environ. Geochem. Health 43, 4235–4249. https://doi.org/10.1007/s10653-021-00919-w.

Hossain, M.B., Tanjin, F., Rahman, M.S., Yu, J., Akhter, S., Noman, M.A., Sun, J., 2022. Metals bioaccumulation in 15 commonly consumed fishes from the lower Meghna river and adjacent areas of Bangladesh and associated human health hazards. Toxics 10 (3), 139. https://doi.org/10.3390/toxics10030139.

Hossain, M.S., Majumder, A.K., 2018. Impact of climate change on agricultural production and food security: a review on coastal regions of Bangladesh. Int. J. Agric. Res. Innov. Technol. 8 (1), 62–69.

Hu, B., Jia, X., Hu, J., Xu, D., Xia, F., Li, Y., 2017. Assessment of heavy metal pollution and health risks in the soil-plant-human system in the Yangtze River Delta, China. Int. J. Environ. Res. Public Health 14 (9), 1042. https://doi.org/10.3390/ijerph14091042.

Islam, F., Parvin, A., Parvin, A., Akhtar, U.S., Shaikh, M.A.A., Uddin, M.N., Moniruzzaman, M., Saha, B., Khanom, J., Suchi, P.D., Hossain, M.A., Hossain, M.K., 2023. Sediment-bound hazardous trace metals (oid) in south-eastern drainage system of Bangladesh: first assessment on human health. Heliyon 9 (9), e20040. https://doi.org/10.1016/j.heliyon.2023.e20040.

Islam, M.S., Proshad, R., Ahmed, S., 2018a. Ecological risk of heavy metals in sediment of an urban river in Bangladesh. Hum. Ecol. Risk Assess. (HERA) 24 (3), 699–720. https://doi.org/10.1080/10807039.2017.1397499.

Islam, M.S., Hossain, M.B., Matin, A., Sarker, M.S.I., 2018b. Assessment of heavy metal pollution, distribution and source apportionment in the sediment from Feni River estuary, Bangladesh. Chemosphere 202, 25–32. https://doi.org/10.1016/j.chemosphere.2018.03.077.

Jiang, J., Wang, J., Liu, S., Lin, C., He, M., Liu, X., 2013. Background, baseline, normalization, and contamination of heavy metals in the Liao River Watershed sediments of China. J. Asian Earth Sci. 73, 87–94. https://doi.org/10.1016/j.jseaes.2013.04.014.

Jolly, Y.N., Rakib, M.R.J., Kumar, R., Islam, A.R.M.T., Rabby, A., Mamun, K.M., Akter, S., Kabir, J., Bhuiyan, T.J., Chowdhury, A.M.S., Idris, A.M., 2023. Deciphering the source of heavy metals in industrially affected river sediment of Shitalakshya river, Bangladesh, and potential ecological and health implications. J. Hazard Mater. Adv. 10, 100268 https://doi.org/10.1016/j.hazadv.2023.100268.

Karmaker, K.D., Hasan, M., Parvin, Afroza, Parvin, Afsana, Hossain, M.S., Rahman, M., Shaikh, M.A.A., Haque, M.I.-M., Hossain, M.K., 2024. Holistic perilous index-based environmental appraisal of Metal(oid)s in the sole coral-bearing island of northeastern bay of Bengal. Chemosphere 359, 142245. https://doi.org/10.1016/j.chemosphere.2024.142245.

Ke, X., Gao, L., Huang, H., Kumar, S., 2015. Toxicity identification evaluation of sediments in Liaohe River. Mar. Pollut. Bull. 93 (1–2), 259–265. https://doi.org/10.1016/j.marpolbul.2015.01.020.

Kükrer, S., Seker, S., Abacı, Z.T., Kutlu, B., 2014. Ecological risk assessment of heavy metals in surface sediments of northern littoral zone of Lake Çıldır, Ardahan, Turkey. Environ. Monit. Assess. 186, 3847–3857. https://doi.org/10.1007/s10661-014-3662-4.

Li, H.B., Yu, S., Li, G.L., Liu, Y., Yu, G.B., Deng, H., Wu, S.C., Wong, M.H., 2012. Urbanization increased metal levels in lake surface sediment and catchment topsoil of waterscape parks. Sci. Total Environ. 432, 202–209. https://doi.org/10.1016/j.scitotenv.2012.05.100.

Li, Z., Ma, Z., van der Kuijp, T.J., Yuan, Z., Huang, L., 2014. A review of soil heavy metal pollution from mines in China: pollution and health risk assessment. Sci. Total Environ. 468, 843–853. https://doi.org/10.1016/j.scitotenv.2013.08.090.

Lu, J., Li, A., Huang, P., 2017. Distribution, sources and contamination assessment of heavy metals in surface sediments of the South Yellow Sea and northern part of the East China Sea. Mar. Pollut. Bull. 124, 470–479. https://doi.org/10.1016/j.marpolbul.2017.07.007.

Ma, W., Tai, L., Qiao, Z., Zhong, L., Wang, Z., Fu, K., Chen, G., 2018. Contamination source apportionment and health risk assessment of heavy metals in soil around municipal solid waste incinerator: a case study in North China. Sci. Total Environ. 631-632, 348–357. https://doi.org/10.1016/j.scitotenv.2018.03.011.

Maanan, M., Saddik, M., Maanan, M., Chaibi, M., Assobhei, O., Zourarah, B., 2015. Environmental and ecological risk assessment of heavy metals in sediments of Nador lagoon, Morocco. Ecol. Indic. 48, 616–626. https://doi.org/10.1016/j.ecolind.2014.09.034.

MacDonald, D.D., Ingersoll, C.G., Berger, T.A., 2000. Development and evaluation of consensus-based sediment quality guidelines for freshwater ecosystems. Arch. Environ. Contam. Toxicol. 39, 20–31. https://doi.org/10.1007/s002440010075.

Mirza, R., Moeinaddini, M., Pourebrahim, S., Zahed, M.A., 2019. Contamination, ecological risk and source identification of metals by multivariate analysis in surface sediments of the Khouran Straits, the Persian Gulf. Mar. Pollut. Bull. 145, 526–535. https://doi.org/10.1016/j.marpolbul.2019.06.028.

Mo, Z., Qin, J., Li, Q., Wei, Y., Ma, S., Xiong, Y., Zou, Y., 2015. Change of water sources reduces health risks from heavy metals via ingestion of water, soil, and rice in a riverine area, South China. Sci. Total Environ. 530, 163–170. https://doi.org/10.1016/j.scitotenv.2015.05.100.

Müller, G., 1969. Index of geoaccumulation in the sediments of the Rhine River. Geojournal 2, 108–118.

Papillomaviruses, H., 2011. IARC Monographs on the Evaluation of Carcinogenic Risks to Humans. IARC, Lyon, France.

Parvin, A., Hossain, M.K., Shahjadee, U.F., Lisa, S.A., Uddin, M.N., Shaikh, M.A.A., Parvin, A., Moniruzzaman, M., Saha, B., Suchi, P.D., 2023. Trace metal exposure and human health consequences through consumption of market-available Oreochromisniloticus (L.) in Bangladesh. Environ. Sci. Pollut. Res. 30 (15), 45398–45413. https://doi.org/10.1007/s11356-023-25414-w.

Rakib, R.J., Hossain, M.B., Jolly, Y.N., Akther, S., Islam, S., 2021. EDXRF detection of trace elements in salt marsh sediment of Bangladesh and probabilistic ecological risk assessment. Soil Sediment Contam. 31 (2), 220–239. https://doi.org/10.1080/15320383.2021.1923644.

Rani, S., Ahmed, M.K., Xiongzhi, X., Keliang, C., Islam, M.S., Habibullah-Al-Mamun, M., 2021. Occurrence, spatial distribution and ecological risk assessment of trace elements in surface sediments of rivers and coastal areas of the East Coast of Bangladesh, North-East Bay of Bengal. Sci. Total Environ. 801, 149782 https://doi.org/10.1016/j.scitotenv.2021.149782.

Sekhar, K.C., Chary, N.S., Kamala, C.T., Raj, D.S., Rao, A.S., 2004. Fractionation studies and bioaccumulation of sediment-bound heavy metals in Kolleru lake by edible fish. Environ. Int. 29 (7), 1001–1008. https://doi.org/10.1016/S0160-4120(03)00094-1.

Shorna, S., Quraishi, S.B., Hosen, M.M., Hossain, M.K., Saha, B., Hossain, A., Habibullah-Al-Mamun, M., 2021. Ecological risk assessment of trace metals in sediment from the old Brahmaputra River in Bangladesh. Chem. Ecol. 37 (9–10), 809–826. https://doi.org/10.1080/02757540.2021.1989422.

Soares, H.M.V.M., Boaventura, R.A.R., Machado, A.A.S.C., da Esteves Silva, J.G.G., 1999. Sediments as monitors of heavy metal contamination in the Ave river basin (Portugal): multivariate analysis of data. Environ. Pollut. 105 (3), 311–323. https://doi.org/10.1016/S0269-7491(99)00048-2.

Sungur, A., Özcan, H., 2015. Chemometric and geochemical study of the heavy metal accumulation in the soils of a salt marsh area (Kavak Delta, NW Turkey). J. Soil. Sediment. 15, 323–331. https://doi.org/10.1007/s11368-014-1013-2.

Suresh, G., Ramasamy, V., Meenakshisundaram, V., Venkatachalapathy, R., Ponnusamy, V., 2011. Influence of mineralogical and heavy metal composition on natural radionuclide concentrations in the river sediments. Appl. Radiat. Isot. 69 (10), 1466–1474. https://doi.org/10.1016/j.apradiso.2011.05.020.

Tomlinson, D.L., Wilson, J.G., Harris, C.R., Jeffrey, D.W., 1980. Problems in the assessment of heavy-metal levels in estuaries and the formation of a pollution index. Helgolander Meeresunters 33, 566–575. https://doi.org/10.1007/BF02414780.

Turekian, K.K., Wedepohl, K.H., 1961. Distribution of the elements in some major units of the earth's crust. Geol. Soc. Am. Bull. 72 (2), 175–192. https://doi.org/10.1130/0016-7606(1961)72[175:DOTEIS]2.0.CO;2.

USEPA, 2004. Risk assessment guidance for superfund. In: Volume I: human health evaluation manual (Part E). EPA/540/R/99/005 OSWER 9285.7-02EP PB99-963312.

USEPA 2011. Regional screening level (RSL) summery table. Washington, DC, USA. Available online: https://epa-prgs.ornl.gov/chemicals/download/master_sl_table_run_JUN2011.pdf (accessed on 5 December 2021).

Wang, X., Zhang, C., Li, S., Wang, C., Wang, H., Cui, Y., 2021. Ecological risk, health risk assessment, and pollution source analysis of Xinli Lake wetland based on triangular fuzzy number. Environ. Sci. Pollut. Res. 28, 22334–22347. https://doi.org/10.1007/s11356-020-12301-x.

Yin, S., Feng, C., Li, Y., Yin, L., Shen, Z., 2015. Heavy metal pollution in the surface water of the Yangtze estuary: a 5-year follow-up study. Chemosphere 138, 718–725. https://doi.org/10.1016/j.chemosphere.2015.07.060.

Zahra, A., Hashmi, M.Z., Malik, R.N., Ahmed, Z., 2014. Enrichment and geo-accumulation of heavy metals and risk assessment of sediments of the KurangNallah—feeding tributary of the Rawal Lake Reservoir, Pakistan. Sci. Total Environ. 470, 925–933. https://doi.org/10.1016/j.scitotenv.2013.10.017.

Zhang, G., Bai, J., Xiao, R., Zhao, Q., Jia, J., Cui, B., Liu, X., 2017. Heavy metal fractions and ecological risk assessment in sediments from urban, rural and reclamation-affected rivers of the Pearl River estuary, China. Chemosphere 184, 278–288. https://doi.org/10.1016/j.chemosphere.2017.05.155.

Zhao, X.M., Yao, L.A., Ma, Q.L., Zhou, G.J., Wang, L., Fang, Q.L., 2018. Distribution and ecological risk assessment of cadmium in water and sediment in Longjiang River, China: implication on water quality management after pollution accident. Chemosphere 194, 107–116. https://doi.org/10.1016/j.chemosphere.2017.11.127.

Zheng, N., Wang, Q.C., Liang, Z.Z., Zheng, D.M., 2008. Characterization of heavy metal concentrations in the sediments of three freshwater rivers in Huludao City, Northeast China. Environ. Pollut. 154 (1), 135–142. https://doi.org/10.1016/j.envpol.2008.01.001.

Zheng, N., Liu, J., Wang, Q., Liang, Z., 2010. Health risk assessment of heavy metal exposure to street dust in the zinc smelting district, Northeast of China. Sci. Total Environ. 408, 726–733. https://doi.org/10.1016/j.scitotenv.2009.10.075.